Lasers Med Sci (2010) 25:283–292
DOI 10.1007/s10103-009-0740-x

ORIGINAL ARTICLE

Zinc phthalocyanine-loaded PLGA biodegradable nanoparticles for photodynamic therapy in tumor-bearing mice

Maha Fadel · Kawser Kassab · Doa Abdel Fadeel

Received: 24 July 2009 / Accepted: 27 October 2009 / Published online: 3 December 2009

Abstract Nanoparticles formulated from the biodegradable copolymer poly(lactic-coglycolic acid) (PLGA) were investigated as a drug delivery system to enhance tissue uptake, permeation, and targeting of zinc(II) phthalocyanine (ZnPc) for photodynamic therapy. Three ZnPc nanoparticle formulations were prepared using a solvent emulsion evaporation method and the influence of sonication time on nanoparticle shape, encapsulation and size distribution, in vitro release, and in vivo photodynamic efficiency in tumor-bearing mice were studied. Sonication time did not affect the process yield or encapsulation efficiency, but did affect significantly the particle size. Sonication for 20 min reduced the mean particle size to 374.3 nm and the in vitro release studies demonstrated a controlled release profile of ZnPc. Tumor-bearing mice injected with ZnPc nanoparticles exhibited significantly smaller mean tumor volume, increased tumor growth delay and longer survival compared with the control group and the group injected with free ZnPc during the time course of the experiment. Histopathological examination of tumor from animals treated with PLGA ZnPc showed regression of tumor cells, in contrast to those obtained from animals treated with free ZnPc. The results indicate that ZnPc encapsulated in PLGA nanoparticles is a successful delivery system for improving photodynamic activity in the target tissue.

Keywords PLGA · Nanoparticles · Zinc phthalocyanine · PDT

M. Fadel
Pharmaceutical Technology Laboratory,
Medical Laser Applications Department,
National Institute of Laser Enhanced Science, Cairo University,
Cairo, Egypt

K. Kassab · D. Abdel Fadeel
Cell Photosensitization and Photobiology Laboratory,
Medical Laser Applications Department,
National Institute of Laser Enhanced Science, Cairo University,
Cairo, Egypt

M. Fadel (✉)
5 El Obour Buildings. Salah Salem St,
Nasr City, Cairo, Egypt
e-mail: mahafmali@hotmail.com

Introduction

Photodynamic therapy (PDT) is a promising novel therapeutic method for the treatment of many tumors. It utilizes a photosensitizer, appropriate wavelength for photoexcitation and oxygen to produce singlet oxygen and other reactive oxygen species, leading to lipid peroxidation, photooxidation of DNA guanine and damage to membranes, cytoskeleton and other sites, and eventual cell death [1].

The first and still frequently clinically approved photosensitizer is the hematoporphyrin derivative Photofrin, which has, however, several drawbacks. Firstly, its longest wavelength absorption maximum is around 630 nm where the penetration depth of light into soft tissues is quite small. Secondly, it is not a pure compound but a mixture of porphyrin dimers and oligomers. Finally, it causes prolonged skin photosensitivity after treatment. Since the photosensitizer is a key element in PDT, there has been a continuous active search for new photosensitizers which could optimize the tumor response to PDT and minimize the side effects and limitations of Photofrin [2]. Zinc(II) phthalocyanine is a second generation photosensitizer which, besides its chemical purity and high singlet oxygen quantum yield, has absorption Q bands at longer wavelengths (around 670 nm) where there is maximum

penetration of light into tissues. Pronounced hydrophobicity characterizes most photosensitizers. This property is considered to be one of the factors responsible for the affinity of the photosensitizer for neoplastic tissues. However, it leads to poor solubility of the molecules in physiologically compatible solvent media, and thus they must be administered in vivo by means of delivery systems [3].

The delivery of hydrophobic photosensitizers is quite challenging. Some drug delivery systems have been developed to deliver photosensitizers such as, liposomes [4], polymeric micelles [5], Cremophor emulsion [6], microspheres and nanoparticles [7]. Increasing attention has focused on formulating therapeutic agents in biodegradable polymeric nanoparticles. Poly(lactic-coglycolic acid) (PLGA) and its derivatives have been the focus for developing nanoparticles encapsulating therapeutic drugs for controlled release applications [8]. The incorporation of photosensitizer into nanoparticles has been shown to reduce toxicity, provide solubility in plasma [9], enhance therapeutic activity [7, 10], prolong the delivery and, in some cases, provide targeting to specific tissues [11]. Moreover, the duration and levels of drug released from the nanoparticles can be easily modulated by altering the formulation parameters such as drug:polymer ratio, and polymer molecular weight and composition [8].

The aim of this study was to examine and evaluate the efficiency of biodegradable polymeric nanoparticles as vehicles for photosensitizer and evaluate the photodynamic activity in vivo. The photosensitizer used was zinc phthalocyanine (ZnPc), a second generation photosensitizer. PLGA nanoparticles loaded with ZnPc were prepared by solvent emulsion evaporation and were characterized in terms of encapsulation efficiency, particle size and in vitro release properties, and finally were tested for their in vivo photodynamic efficiency using mice bearing tumor.

Materials and methods

Laboratory studies

Materials

Zinc(II) phthalocyanine (ZnPc, MW 577.91 Da), poly (D,L-lactic-coglycolic acid) (PLGA 50:50, MW 40,000–75,000 Da), polyvinyl alcohol (PVA) and HEPES buffer (*N*-[2-hydroxyethyl] piperazine-*N*′-[2-ethanesulfonic acid]) were purchased from Sigma Aldrich (St Louis, MO). Sodium dodecyl sulfate (SDS), lactose, dichloromethane (DCM) and pyridine, all of analytical grade,+ were purchased from El Nasr Pharmaceutical Chemicals (Adwic, Egypt).

Preparation of ZnPc-loaded PLGA nanoparticles

ZnPc-loaded PLGA nanoparticles were prepared by solvent emulsion evaporation as described previously [11]. In this study the effect of sonication time on the physiochemical properties of the nanoparticles was studied. Three formulations were prepared with different sonication times of 5, 10, and 20 min (formulation A, B, and C, respectively). Briefly, the organic phase of 40 mg PLGA and 0.25 mg ZnPc in 4 ml DCM was added drop-wise to a solution of PVA (3%, w/w) while mixing in Ultraturrax T25 laboratory emulsifier (Ika, Staufen, Germany) at 20,500 rpm. The resulting emulsion was sonicated using a Retsch sonicator at 80 W output (Retsch, Haan, Germany). The solvent (DCM) was evaporated at room temperature (25°C) for 5 h, under magnetic stirring in the dark. ZnPc-loaded nanoparticles were purified by 30 min centrifugation at 5,000 rpm and resuspended in water containing 5% lactose (lyoprotectant). Finally, the nanoparticles were freeze-dried using a 4.5-l Lyph-Lock freeze-drying system (Labconco Corporation, Kansas City, MO) yielding powdered nanoparticles which were stored at 4°C to be used for further analysis.

Process yield

The process yield was expressed as percentage of the total mass of nanoparticles obtained after freeze drying relative to the weight of the initial drug plus polymer. It was calculated as:

$$Y(\%) = M_{NP}/M_T \times 100 \quad (1)$$

Where Y(%) is the process yield, M_{NP} is the mass of PLGA plus the mass of nanoparticles recovered after freeze drying and M_T is the mass of PLGA plus the mass of ZnPc in the formulation. This procedure was carried out for each formulation in triplicate (n=3).

ZnPc encapsulation efficiency

Freeze-dried nanoparticles (10 mg) of each formulation were dissolved in 10 ml pyridine, and aliquots of 0.5 ml were diluted with HEPES buffer containing 2% SDS and magnetically stirred for 1 h at 25°C. The suspension obtained was centrifuged at 10,000 rpm for 10 min and the ZnPc content in the supernatant was measured by spectrofluorimetry using a Shimadzu 1501-RF spectrofluorimeter (Shimadzu, Kyoto, Japan), setting the excitation wavelength at 610 nm and monitoring the emission n the range 650–800 nm. The concentration of ZnPc was calculated by means of a standard calibration curve derived for known concentrations of ZnPc

(0.0097–2.5 μg/ml) vs. the area of fluorescence emission. Precision and linearity were calculated from the coefficient of variation and linear regression of the standard curve, respectively [5].

The encapsulation efficiency was calculated from the following equation:

$$EE = M_1/M_T \times 100 \quad (2)$$

Where EE is the ZnPc encapsulation efficiency, M_1 the mass of ZnPc in the nanoparticles, and M_t the mass of ZnPc used in the formulation. The experiments were carried out in triplicate for each formulation (n=3).

In vitro release kinetic analysis

The release study was performed under sink conditions as described previously [11–14]. Briefly, freeze-dried nanoparticles (15 mg, equivalent to 10 μg ZnPc of each formulation) were dispersed in 50 ml HEPES buffer containing 2% SDS, pH 7.4, and adjusted to 37°C. The acceptor solution was stirred with a paddle at a constant rate of 100 rpm, using dissolution apparatus (model TDT-08L; Electrolab, Mumbai, India) in the dark. The paddles were fitted to 100-ml glass dissolution vessels. At 24-h intervals, 3-ml aliquots were withdrawn and centrifuged at 10,000 rpm for 10 min. The precipitates were resuspended in 3 ml of fresh medium and placed in the acceptor solution again. Fluorescence emission spectra of the supernatant were measured under the conditions described above, and the areas of the spectra were utilized to calculate the concentrations of ZnPc released from the PLGA nanoparticles (n=3).

To study the mechanism of ZnPc release from the three formulations the data were fitted to zero, first, and Higuchi's diffusion control models using coefficient of variation for data analysis StatistiXL for MS Excel software. The release kinetics were estimated by applying the highest linear correlation coefficient and the lowest coefficient of variation.

Particle size analysis

The mean particle size and size distribution of each formulation were measured by laser light scattering using a particle size analyzer (Zetasizer, Malvern, UK). Size measurements were performed following a 1/10 (v/v) dilution of the nanoparticle suspension in distilled water. The size distribution was analyzed over the range 1–3000 nm and the mean diameter was calculated for each sample. The nanoparticle suspension was measured in a capillary cell (detector angle 90°, at 25°C, wavelength 633 nm) with 24 readings taken for each sample.

Scanning electron microscopy

Freeze-dried particles were viewed by scanning electron microscopy to examine their morphology. Dried nanoparticles were prepared on glass slides, coated with gold, and then examined by scanning electron microscopy (100 S; JEOL, Tokyo, Japan).

In vivo animal study

Animals and tumor implantation

All animal experiments were performed following the 'Principles of laboratory animal care' (NIH publication no. 85-23, revised 1985), as well as specific institutional laws on 'protection of animals' under the supervision of authorized investigators. Ehrlich ascites carcinoma cells were kindly supplied by the National Institute of Cancer Research, Cairo University. The study animals comprised 65 female albino mice of average weight 20±3 g. The mice were housed at room temperature with a regular light/dark cycle and free access to food and water. A group of 5 animals were kept healthy and the other 60 animals were injected in the thigh of the hind limb, each with 2×10^6 Ehrlich ascites carcinoma cells in 0.2 ml normal saline.

PDT protocol

Since the three prepared formulations (A, B, and C) differed significantly only in particle size, formulation C with the lowest particle size was used in the in vivo study. The treatment protocol started with intralesional injection on the 8th day after tumor implantation. The animals injected with tumor cells were subdivided into four groups each comprising 15 animals as follows:

- Control group: animals did not receive any treatment,
- LED group: animals received 120 J/cm^2 red light only from a LED type gallium midi-33 diode cluster system (Sim-med, Billingshurst, UK).
- FZnPc group: animals injected with a sterile solution of free ZnPc (0.8 μg ZnPc/kg body weight) in 0.3% SDS.
- NZnPc group: animals injected with freeze-dried (0.8 μg ZnPc/kg body weight) nanoparticles in normal saline, and 24 h after injection tumors were irradiated under the same conditions (distance from light source and spot size) with a LED at 100 mW/cm^2 for 20 min.

Evaluation of the effect of PDT

The effect of PDT on the tumors in the different animal groups was evaluated by measurement of tumor volume, by

determination of tumor growth delay (TGD) and survival, and by histopathological examination of tumor specimens.

Tumor volume measurements The tumor growth was followed by measuring the three mutually orthogonal tumor diameters with a caliper. The tumor volume was calculated from the equation: $V = \pi/6(a \times b \times c)$, where V is the tumor volume (in cubic centimeters), and a, b and c are the orthogonal dimensions of the tumor (in centimeters). Tumors volumes were measured weekly and the changes in volume are represented as the means±SD.

Tumor growth delay PDT was initiated when the tumor volume was approximately 0.15 cm^3. The change in volume of the tumor in each animal was determined weekly until the volume reached 2 cm^3. TGD was calculated as the additional time in days taken by the tumor in each animal in the treated groups to reach 2 cm^3 beyond that required in the untreated control group.

Survival assay The day of death of every mouse was recorded and the percent of surviving animals in each group was calculated. The experiment was terminated 80 days after tumor implantation.

Histopathological examination Three mice from the control group were killed by an overdose of general anesthetic 7 days after tumor implantation. Three mice each from the LED, FZnPc and NZnPc groups were killed at 7, 15 and 21 days after PDT, respectively. The tumor tissues were excised, fixed in 10% formalin and embedded in paraffin. The blocks were cut at a thickness of 3 μm, stained with hematoxylin and eosin and pathologically examined under an optical microscope type BML 2200 (Biomed, Laborgeräte; made in Japan) attached to a color CCTV camera (WV-CP 240/G; Panasonic System Solution Suzhou, Suzhou, China).

Data analyses

One-way analysis of variance and the Tukey-Kramer multiple comparisons test were used to determine the significance of differences in encapsulation efficiency, release data and tumor size. All *p*-values are two-tailed, and differences are considered significant when the *p*-value is less than 0.05 and considered highly significant when the *p*-value is less than 0.01. The final data are expressed as means±SD.

Results

Evaluation of the method of preparation, process yield and encapsulation efficiency

To determine the influence of sonication time on nanoparticle shape, encapsulation and size distribution, three formulations were prepared, A, B and C, with sonication time of 5, 10 and 20 min, respectively. As shown in Table 1, the sonication time did not significantly affect the process yield or the encapsulation efficiency ($p \geq 0.05$). The slight decrease in the encapsulation efficiency on increasing the sonication time is due to the decrease in particle size, i.e. larger particles had higher encapsulation efficiency. This is consistent with the results obtained by Song et al. [15], who suggested that the increase in nanoparticle size could increase the length of the diffusional pathway of the drug from the organic phase to the aqueous phase, thereby reducing drug loss through diffusion and increasing drug entrapment efficiency.

Particle size and particle size distribution

The particle size and size distribution for each formulation were measured by laser light scattering (Table 1). The size of the prepared particles was in the nanometer range with a wide distribution. Among the three formulations, formulation C, with 20 min sonication, had significantly ($p \leq 0.05$) the lowest mean particle size (374.3±5.6 nm) and exhibited a unimodal size distribution. Increasing the sonication time reduced the mean diameter of the nanoparticles and changed the population distribution from bimodal for formulation A (diameter 830.2±4.2 nm) and formulation B (diameter 419.6±4.6 nm) to the unimodal mode with a polydispersity index of 1, where nearly 85% of the particles had a size range between 227 and 450 nm.

Scanning electron microscopy

Based on the images obtained by electron microscopy, the three formulations showed no morphological differences.

Table 1 The process yield, encapsulation efficiency and the mean particles diameter of the three formulations

Formulation	Sonication time (min)	Yield (%)	Encapsulation efficiency (%)	Diameter (nm)
A	5	86±3.2	84±2	830.2±111
B	10	85±3.1	82±2.1	419.6±87
C	20	85±3.3	80±2.3	347.3±56

As shown in Fig. 1, all the obtained nanoparticles were spherical in shape with a smooth surface.

In vitro release study

The in vitro release of ZnPc from PLGA nanoparticles was studied. The nanoparticles were suspended directly in HEPES buffer containing 2% SDS as an acceptor medium. The cumulative percentage of drug release profile from the three formulations is shown in Fig. 2. The release profiles did not show significant difference and all exhibited an initial burst release of 10% for 3 days followed by controlled release which was best fitted with zero-order kinetics (r^2=0.98±0.002) with an insignificant difference in release rate (p>0.05) between the formulations (release rate K_0=0.3±0.011) for a short period of 21 days. Such a relatively short period could be an advantage in avoiding prolonged photosensitivity, and the kinetic release (zero-order) reflects a sustained PLGA degradation and subsequent ZnPc release.

In vivo study

Tumor volume measurements

Tumor volumes were measured weekly as described above and the changes in tumor volume are represented as mean±SD as shown in Fig. 3. Eight days after tumor inoculation, the tumor volume was approximately 0.15± 0.02 cm^3 in all groups. By 1 week after treatment (15 days after tumor inoculation), the mean tumor volume in the control group and LED group (1.36 cm^3) was significantly larger (p<0.05) than in the FZnPc group (0.68 cm^3) and NZnPc group (0.64 cm^3). By 2 weeks after treatment, all the mice in the control group and LED group had died and the mean tumor volume in the NZnPc group (0.81 cm^3) was significantly less (p<0.05) than in the FZnPc group (1.19 cm^3). One week later, all the mice that had received free ZnPc were dead, and those that had received PLGA ZnPc nanoparticles remained alive for an additional 8 weeks, after which they were killed by an overdose of general anesthetic because of ethical concerns.

Tumor growth delay

The tumor volume in both the control and LED groups had reached 2 cm^3 at 18±2 and 18±1 days after tumor inoculation, respectively. The same volume was attained at 27 days in the FZnPc group (TGD 9±0.3 days), and at 56 days in the NZnPc group (TGD 48±0.34 days). The difference between the mean TGD in the NZnPc group and the FZnPc group was highly significant (p=0.01).

Survival assay

In this experiment, the number of animals surviving from each group after tumor inoculation was determined as a function of incubation period. Figure 4 illustrates the variation in animal survival percentage as a function of incubation period following tumor inoculation and the mean survival time of each group. The mean survival time in the control group (15.75 days) was significantly shorter (p<0.05) than in the FZnPc and NZnPc groups. On the other hand, the mean survival time in the NZnPc group (60 days) was significantly longer (p=0.029) than in the FZnPc group (25 days). At 80 days after tumor implantation, 20% of mice that had received NZnPc were still alive, while all the animals that had received FZnPc were dead by day 30. The results of the survival assay are in agreement with the TGD results.

Histopathological examination

Three mice of the control group were killed 7 days after tumor implantation. Three mice each from the LED, FZnPc and NZnPc groups were killed at 7, 15 and 21 days after PDT, respectively. Figure 5 shows representative histopathological sections from each group. The lesional muscle of mice from the control group and LED group (Fig. 5a, b) showed microscopic islands of malignant cells deep in

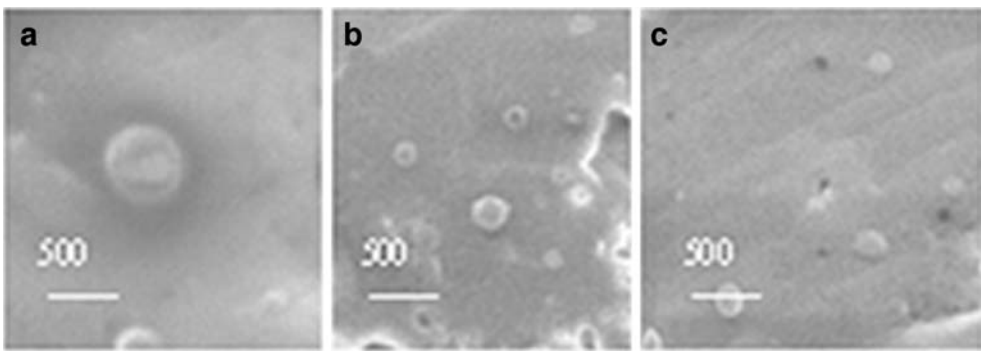

Fig. 1 Scanning electron micrographs of the three formulations A, B and C (×2,000)

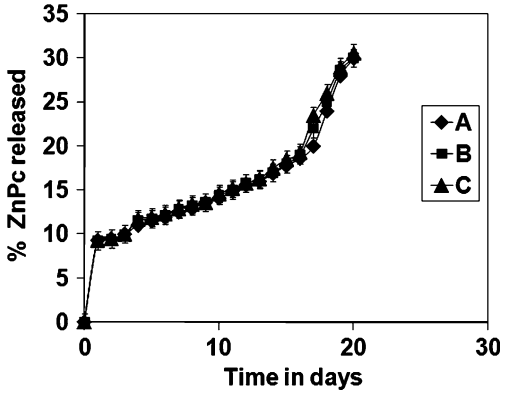

Fig. 2 In vitro drug release profile from formulations A, B and C as a function of time in days

between the muscle bundles surrounded by strands of connective tissue and vascularized stroma. The neoplastic cells had hyperchromatic and pleomorphic nuclei and scant eosinophilic cytoplasm, were arranged in sheets, and varied in size and shape.

The FZnPc group 2 weeks after treatment (Fig. 5c) showed evident vacuolation in the sarcoplasm of lesional muscle in between muscle bundles and inside islands of tumor cells. The coagulated necrotic masses showed closely packed, degenerated tumor cells with scattered and degenerated inflammatory cells. On the other hand, after 3 weeks lesional muscle from the NZnPc group showed a few islands of aggregates of neoplastic cells. These cells varied in size and shape. Large islands of normal muscle tissue were seen in between the aggregates of tumor cells and islands of necrotic cells were seen (Fig. 5d).

Discussion

ZnPc-loaded PLGA nanoparticles were prepared successfully by solvent emulsion evaporation as described previously [11, 15]. Although the method is conceptually simple, many factors have been shown to influence the final characteristics of the resultant PLGA nanoparticles [16].

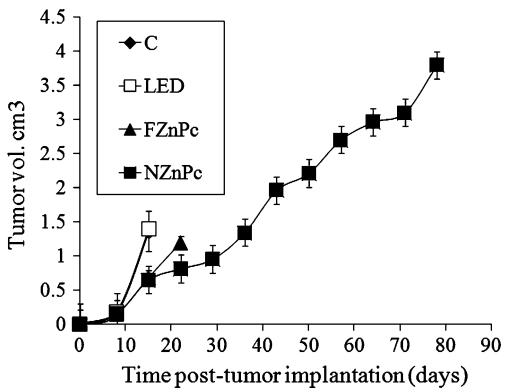

Fig. 3 Tumor volumes in the different groups as a function of days after tumor implantation

DCM was used as organic solvent since it is widely used for drug encapsulation into polymeric nanoparticles [17]. PVA is the emulsifier most commonly used to stabilize the emulsion since it forms particles of relatively small size and uniform size distribution [18].

The influence of sonication time on the shape, encapsulation and size distribution of the nanoparticles was studied. Three similar formulations were prepared differing only in the sonication time. Under all conditions, a high yield and encapsulation efficiency of ZnPc were obtained. In general, efficient encapsulation of hydrophobic drugs, such as ZnPc, into hydrophobic polymers such as PLGA, is relatively easy, as the limited water solubility of the drug suppresses its tendency to escape out of nanoparticles into the aqueous phase during the formulation process, which is a behavior opposite to that observed in the case of hydrophilic drugs [19].

While prolonging the sonication time did not affect the process yield, the encapsulation efficiency slightly decreased. The decrease in encapsulation efficiency with sonication time can be explained in terms of the effect of sonication time on particle size. In fact, prolonged sonication reduced the mean diameter of the nanoparticles and changed the population distribution from bimodal to unimodal. Our results are consistent with those obtained by Song et al. [20] who studied the effect of many preparation variables on the mean diameter of PLGA and found that the mean diameter increases with increasing concentration and molecular weight of PLGA and decreases with increasing PVA concentration, removal rate of organic solvent and sonication time, but with a further increase in sonication time, the particle size reaches a plateau.

A study of the effect of formulation variables on the size distribution of PLGA nanoparticles containing prazequantal showed that the final size of the nanoparticles depends on the globule size throughout the emulsification process. A reduction in the emulsion globule size allows the formation of smaller nanoparticles [21]. An increase in sonication duration increases the energy causing droplet breakdown, which in turn increases the shear stress resulting in decreased particle size. In addition, studies of other processing parameters such as polymer concentration in the organic phase, initial drug concentration in the organic phase, solvent volume, PVA concentration in the aqueous phase and the aqueous phase volume, have revealed that the same factors could be applied to any hydrophobic drug–polymer system produced by the solvent emulsion evaporation method [22]. These factors were applied rationally to produce unimodal particles of various mean sizes (220–1,000 nm). However, at 20 min sonication time, the particle size started to increase again [23].

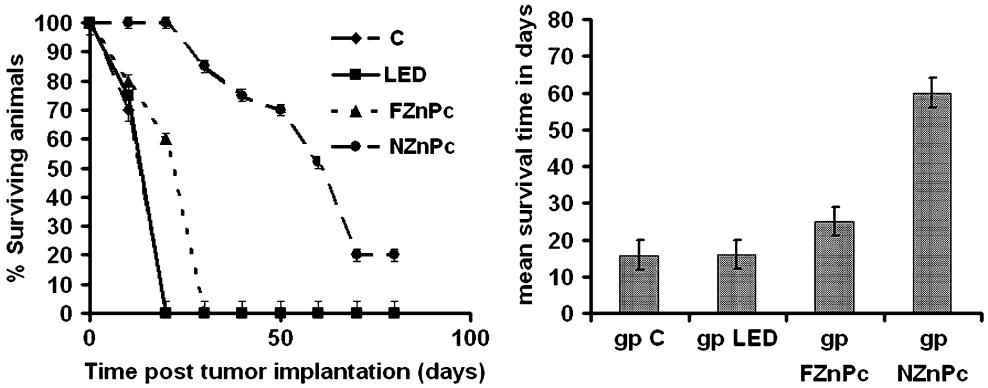

Fig. 4 The percentage of surviving animals in the different groups (*left*) and the mean survival time as a function of incubation period following tumor implantation (*right*)

The in vitro release of ZnPc from PLGA nanoparticles was studied under sink conditions. The nanoparticles were suspended directly in the acceptor medium (HEPES buffer containing 2% SDS) without a membrane or dialysis bag. The same technique was adopted by Pinõn- Segundo et al. [12], Naraharisetti et al. [13] and Wischke and Schwendeman [14]. Our results agree with those of the previous studies which revealed that the difference in particle size and drug content does not significantly affect the release kinetics from nanoparticles [24, 25].

The initial burst release is one of the major persistent problems in the development of injectable polymeric delivery systems [26]. It could be prevented by developing more sophisticated drug delivery systems, such as PLGA nanoparticles [27]. The initial burst release may be due to the drug molecules in the outer layer of PLGA [12]. Our results showed that there is an initial burst release of 10% for 3 days, and then the release rate is very low over a period of 20 days. These results are similar to those obtained by Ricci-Júnior and Marchetti [11] who studied the in vitro release of ZnPc from PLGA nanoparticles and reported that there was an initial burst release of 15% for 3 days, followed by a slow release over a period of 25 days and nearly 40% of ZnPc was released from the PLGA nanoparticles.

Drugs have been considered to be released from PLGA micro- or nanoparticles by the following mechanisms: (a) surface deposition, (b) diffusion through the particle pole, (c) diffusion through the intact polymer, (d) diffusion through a water-swollen polymer, and (e) surface or bulk erosion of polymer matrix. The most important mechanisms are drug diffusion and polymer erosion [28]. If the diffusion of the drug is faster than polymer degradation, then the mechanism of the drug release occurs mainly by diffusion

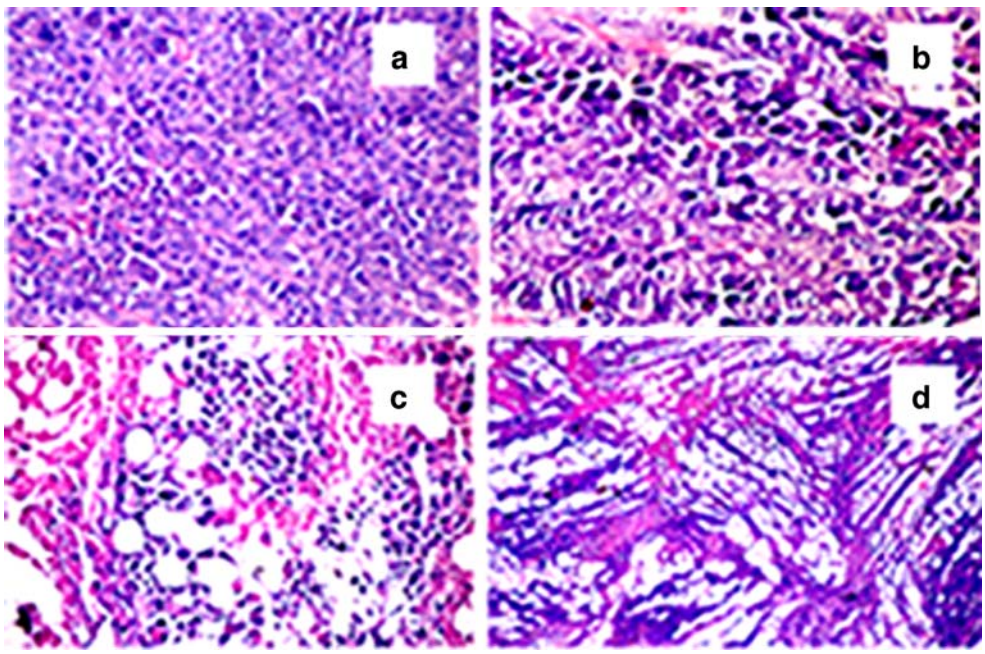

Fig. 5 Representative histological sections of lesional muscle from each group of mice. **a**, **b** Sections from the control group (**a**) and LED group (**b**) show tumor cell islands in between the muscles bundles. **c** Sections from the ZnPc group show vacuolation of the cytoplasm of some tumor cells. **d** Sections from the NZnPc group 30 days after injection show no tumor cells (H&E, ×40)

[29]. The degradation of the polymer shows a clear dependence on the polymer's molecular weight (inherent viscosity). Longer polymers require a longer time to degrade which leads to a longer release time of drug [30]. In our study, a high molecular weight polymer was used (40,000–75,000 Da). This high molecular weight may be responsible for the low burst release and the slow release rate [31]. Finally we can say that the release of ZnPc from PLGA nanoparticles is dependent on many factors, the most important of which are the drug diffusion and the polymer degradation.

To assess the antitumor activity in vivo, PLGA nanoparticles loaded with ZnPc were directly injected into implanted Ehrlich tumors in albino mice. SDS, which is a surface-active agent, was used to disperse free hydrophobic ZnPc in the buffer, without affecting its photodynamic behavior. It has been reported that smaller nanoparticles size are less readily recognized by the reticuloendothelial system, and thus the encapsulated photosensitizer shows greater activity [32]. In a previous in vivo study, m-THPP loaded into three batches of PLGA nanoparticles of different particle sizes (100, 300 and 800 nm) showed less photodynamic activity when incorporated into large nanoparticles than in small nanoparticles [33]. Hence, in this study the formulation with the smallest particle size was chosen for injection into the animals. Based on many previous studies which have shown that the maximum concentration of ZnPc in tumors is reached 24 h after injection [34], tumors were irradiated 24 h after injection with a LED that had been used previously as a light source in PDT [35–39].

The antitumor activity of ZnPc loaded into PLGA nanoparticles was compared with that of free ZnPc dissolved in SDS and with the effect of LED light in the absence of photosensitizer. The three groups were compared with the control tumor-bearing group which did not receive any treatment. There was no significant difference between the LED group and the control group with respect to tumor volume, TGD, survival and histopathological findings. This is consistent with the results of many studies of the in vivo photosensitizing activity of different photosensitizers. These studies have shown that tumor growth progression in mice treated with photosensitizers in the absence of light or irradiated in the absence of photosensitizers is the same as in untreated mice [40].

In the present study, all groups showed an increase in tumor size, but at different rates and to different extents compared with the initial tumor size at the beginning of the experiment. These results agree with those obtained previously with PDT mediated by temoporfin-loaded invasomes in subcutaneously implanted tumors in mice, even after repeated photoirradiation [41]. Our results showed that the tumor volume in animals treated with NZnPc remained the smallest of the three groups during the course of the experiment. This was confirmed by the finding that the animals that received NZnPc exhibited longer TGD and survival than the control ZnPc groups.

On histopathological examination the number of degenerated and necrotic tumor cells was seen to be increased more in the NZnPc group killed 7 days after PDT than in the FZnPc group. The degeneration of tumor was more substantial in the NZnPc group at 15 and 30 days after PDT. At the end of the experiment, the tumor cells had almost vanished.

It is clear from the in vivo study that ZnPc loaded into PLGA nanoparticles was superior to its free form. This is consistent with the results of many studies comparing the outcome of PDT following injection of nanoparticles loaded with photosensitizer and following injection of free photosensitizer under otherwise identical conditions. Such findings provide strong evidence that a nanoparticle formulation achieves improved delivery of photosensitizer to tumor cells for PDT [10, 32, 42, 43]. The development of suitable carriers for hydrophobic photosensitizers is very important because, even if they are dissolved in a solvent tolerable by patients, solvents cause alterations in the drug biodistribution and thereby hamper the targeting and the controlled delivery of drugs [33].

Previous studies on the pharmacokinetics of octa-alpha-butyloxy-ZnPc and hexadecafluoro ZnPc in tumor-bearing mice using 1% Tween 80 and Cremophor emulsion (which has been reported to elicit acute hypersensitivity and anaphylactic reactions in vivo) have shown very low accumulation of the photosensitizer in the tumor, and it was concluded that the photosensitizer must be formulated in a suitable carrier system in order to increase its concentration in the target tissue and decrease its loss to other tissues, and to provide selective sensitivity for PDT [44].

Conclusion

The solvent emulsion evaporation method allowed the preparation of spherical biodegradable PLGA nanoparticles loaded with ZnPc. The efficacy of PDT has been hindered by the inability to deliver the photosensitizers to the tumor at effective concentrations. The nanoparticles approach therefore seems to be a promising strategy to overcome the delivery issues and to enhance the phototherapeutic response during cancer treatment. It increases the solubility and dissolution rate of poorly soluble drugs, allowing sustained drug release and enabling the control of some physical properties, such as drug concentration and particle size.

References

1. Moan J, Berg K (1992) Photo chemotherapy of cancer: experimental research. Photochem Photobiol 55:931–948
2. Dougherty TJ, Gomer CJ, Henderson BW et al (1998) Photodynamic therapy. J Natl Cancer Inst 90(12):889–905
3. Soncin M, Polo L, Reddi E et al (1995) Effect of the delivery system on the biodistribution of Ge(IV) octabutoxy-phthalocyanines in tumour-bearing mice. Cancer Lett 89:101–106
4. Derycke ASL, De Witte VAM (2004) Liposomes for photodynamic therapy. Adv Drug Deliv Rev 56:17–30
5. Sibata MN, Tedesco AC, Marchetti JM (2004) Photophysical and photochemical studies of zinc(II) phthalocyanine in long time circulation micelles for photodynamic therapy use. Eur J Pharm Sci 23:131–138
6. Soncin M, Polo L, Reddi E et al (1995) Unusually high affinity of Zn(II) tetradibenzobarrelenooctabutoxy-phthalocyanine for low density lipoproteins in a tumor-bearing mouse. Photochem Photobiol 61(3):310–312
7. Allémann E, Brasseur N, Benrezzak O et al (1995) PEG-coated poly(lactic acid) nanoparticles for the delivery of hexadecafluoro zinc phthalocyanine to EMT-6 mouse mammary tumours. J Pharm Pharmacol 47(5):382–387
8. Hans ML, Lowman AM (2002) Biodegradable nanoparticles for drug delivery and targeting. Curr Opin Solid State Mater Sci 6 (4):319–327
9. Kawashima Y (2001) Nanoparticulate systems for improved drug delivery. Adv Drug Deliv Rev 47(1):1–2
10. Konan YN, Berton M, Gurney R, Allemann E (2003) Enhanced photodynamic activity of meso-tetra(4-hydroxyphenyl) porphyrin by incorporation into sub-200 nm nanoparticles. Eur J Pharm Sci 18(3–4):241–249
11. Ricci-Júnior E, Marchetti JM (2006) Zinc(II) phthalocyanine loaded PLGA nanoparticles for photodynamic therapy use. Int J Pharm 310:187–195
12. Pinõn-Segundo E, Garnem-Quintanar A, Alonso-Perez V, Quintanar-Guerrerro D (2005) Preparation and characterization of triclosan nanoparticles for periodontal treatment. Int J Pharm 294:217–232
13. Naraharisetti PK, Lew MD, Fu Y, Lee DJ, Wang CH (2005) Gentamicin-loaded discs and microspheres and their modifications: characterization and in vitro release. J Control Release 102 (2):345–359
14. Wischke C, Schwendeman SP (2008) Principles of encapsulating hydrophobic drugs in PLA/PLGA microparticles. Int J Pharm 364:298–327
15. Song CX, Labhasetwar V, Murphy H et al (1997) Formulation and characterization of biodegradable nanoparticles for intravascular local drug delivery. J Control Release 43:197–212
16. Cheng YH, Illum L, Davis SS (1998) A poly(D,L-lactide-co-glycolide) microsphere depot system for delivery of haloperidol. J Control Release 55:203–212
17. Gómez-Gaete C, Tsapis N, Besnard M, Bochot A, Fattal E (2007) Encapsulation of dexamethasone into biodegradable polymeric nanoparticles. Int J Pharm 331:153–159
18. Sahoo SK, Panyam J, Prabha S, Labhasetwar V (2002) Residual polyvinyl alcohol associated with poly(D,L-lactide-co-glycolide) nanoparticles affects their physical properties and cellular uptake. J Control Release 82(4):105–114
19. Kompella UB, Bandi N, Ayalasomeyajula SP (2001) Poly(lactic acid) nanoparticles for sustained release of budesonide. Drug Deliv Technol 1:28–34
20. Song X, Zhao Y, Wu W et al (2008) PLGA nanoparticles simultaneously loaded with vincristine sulfate and verapamil hydrochloride: systematic study of particle size and drug entrapment efficiency. Int J Pharm 350:320–329
21. Mainardes RM, Evangelista RC (2005) PLGA nanoparticles containing prazequantal: effect of formulation variables on size distribution. Int J Pharm 290:137–144
22. Budhian A, Siegal SJ, Winey KI (2007) Haloperidol-loaded PLGA nanoparticles: systematic study of particle size and drug content. Int J Pharm 336:367–375
23. Scholes PD, Coombes AGA, Illum L et al (1993) The preparation of sub-200 nm poly-(lactide-co-glycolide) microspheres for site specific drug delivery. J Control Release 25:145–153
24. Jeong YI, Na HS, Seo DH et al (2008) Ciprofloxacin-encapsulated poly(D,L-lactic-co-glycolic) nanoparticles and its antibacterial activity. Int J Pharm 352:317–323
25. Klosa D, Siepmann F, Elkharraz K, Siepmann J (2008) PLGA-based drug delivery systems: importance of the type of drug and device geometry. Int J Pharm 354:95–103
26. Yeo Y, Park K (2004) Control of encapsulation efficiency and initial burst in polymeric microparticle systems. Arch Pharmacol Res 27:1–12
27. Hasan AS, Socha M, Lamprecht A et al (2007) Effect of the microencapsulation of nanoparticles on the reduction of burst release. Int J Pharm 344:53–61
28. Li X, Deng X, Huang Z (2001) In vitro protein release and degradation of poly-dl-lactide-poly(ethylene glycol) microspheres with entrapped human serum albumin: quantitative evaluation of the factors involved in protein release phases. Pharm Res 18:117–124
29. Soppimath KS, Aminabhaui TM, Kullkarni AR, Rudzinski WE (2001) Biodegradable polymeric nanoparticles as delivery devices. J Control Release 70:1–20
30. Giteau A, Venie-julienne MC, Aubert-Pouëssel A, Benoit JP (2008) How to achieve sustained and complete protein release from PLGA-based microparticles? Int J Pharm 350:14–26
31. Zolnik BS, Leary PE, Burgess DJ (2006) Elevated temperature accelerated release testing of PLGA microspheres. J Control Release 12:293–300
32. Pegaz B, Debefve E, Ballini JP, Konan-Kouakou YN, van den Bergh H (2006) Effect of nanoparticles size on the extravasation and the photothrombic activity of meso(p-tetracarboxyphenyl)porphyrin. J Photochem Photobiol B 85 (3):216–222
33. Vargas A, Eid M, Fanchaouy M, Gurny R, Delie F (2008) In vivo photodynamic activity of photosensitizer-loaded nanoparticles: formulation properties, administration parameters and biological issues involved in PDT outcome. Eur J Pharm Biopharm 69:43–53
34. Milla LN, Yslas EI, Cabral A et al (2008) Pharmacokinetics, toxicological and phototherapeutic studies of phthalocyanine ZnPcCF3. J Biomed Pharmacother 63:209–215
35. Salah M, Samy N, Fadel M (2009) Methylene blue mediated photodynamic therapy for resistant plaque psoriasis. J Drug Dermatol 8:42–49
36. Calista D (2009) Photodynamic therapy for the treatment of a giant superficial basal cell carcinoma. Photodermatol Photoimmunol Photomed 25:53–54
37. Berking C, Hegyi J, Arenberger P, Ruzicka T, Jemec GB (2009) Photodynamic therapy of necrobiosis lipoidica – a multicenter study of 18 patients. Dermatology 218:136–139
38. Pariser D, Loss R, Jarratt M et al (2008) Topical methyl-aminolevulinate photodynamic therapy using red light-emitting diode light for treatment of multiple actinic keratoses: a randomized, double-blind, placebo-controlled study. J Am Acad Dermatol 59:569–576
39. Peloi LS, Soares RR, Biondo CE, Souza VR, Hioka N, Kimura E (2008) Photodynamic effect of light-emitting diode light on

cell growth inhibition induced by methylene blue. J Biosci 33:231–237
40. Karmakova T, Feofanov A, Pankratov A et al (2006) Tissue distribution and in vivo photosensitizing activity of 13,15-[N-(3-hydroxypropyl)]cycloimide chlorin p6 and 13,15-(N-methoxy) cycloimide chlorin p6 methyl ester. J Photochem Photobiol B 82:28–36
41. Dragicevic-Curic N, Gräfe S, Albrecht V, Fahr A (2008) Topical application of temoporfin-loaded invasomes for photodynamic therapy of subcutaneously implanted tumors in mice: a pilot study. J Photochem Photobiol B 91:41–50
42. Ismail MS, Dressler C, Koeppe P et al (1997) Pharmacokinetic analysis of octa-alpha-butyloxy-zinc phthalocyanine in mice bearing Lewis lung carcinoma. J Clin Laser Med Surg 15(4):157–61
43. Pegaz B, Debefve E, Borle F, Ballini JP, van den Bergh H, Kouakou-Konan YN (2005) Encapsulation of porphyrins and chlorins in biodegradable nanoparticles: the effect of dye lipophilicity on the extravasation and the photothrombic activity. A comparative study. J Photochem Photobiol B 80(1):19–27
44. Gelderblom H, Verweij J, Nooter K, Sparreboom A (2001) Cremophor EL: the drawbacks and advantages of vehicle selection for drug formulation. Eur J Cancer 37:1590–1598